Seventh Water Reactor Safety Research Information Meeting

November 5-9, 1979

Recent Results From the NSRR Experiments

M. Ishikawa, T. Fujishiro, T. Hoshi, N. Ohnishi

Reactivity Accident Laboratory
Division of Reactor Safety
Japan Atomic Energy Research Institute

1. Introduction

Since the start of Nuclear Safety Research Reactor (NSRR) Project in October 1975, over 350 tests have been performed to date to study the fuel behavior under simulated reactivity initiated accident (RIA) conditions. Scoping tests and NSRR standard rod tests were conducted in the earliest stage of the project to establish the base line data with the standard rods (PWR type rods). Then, the tests to study the effects of various parameters were initiated. The major parameters chosen are (1) fuel design parameters; i.e. pellet-cladding gap width, fuel enrichment, rod internal pressure, cladding material and gap gas composition, (2) cooling environment parameters; i.e. coolant subcooling, flow shroud, forced convection and rod bundle, (3) defective fuel rods, i.e. waterlogged rods and rods with fretting corroded claddings. The effects of these parameters are being investigated by comparing with the base line data.

Among the standard and the parameter tests mentioned above, NSRR standard rod tests and the tests on fuel design parameters are almost complete and the results were already reported in the former Water Reactor Safety Information Meetings.
The basic conclusions are as follows.

(1) The standard rods failed when the energy deposition exceeded around 260 cal/gUO_2 caused mainly by cladding melting.
No mechanical energy was generated when the energy deposition was below 380 cal/g·UO_2.

(2) Fuel fragmentation occurred at the energy deposition of over 380 cal/g·UO_2 when the gross melting of UO_2 pellet was attained. Mechanical energy generation was observed at this type of failure.

(3) Fuel design parameters except rod internal pressure do not have significant influences on failure mode and threshold energy.

(4) Fuel failure was caused by high temperature burst of the cladding in pre-pressurized rod tests at lower energy depositions than standard rod failure thershold. A large ballooning of cladding was usually observed in this type of failure.

Two new topics are presented in this report; the results of the cooling environment parameter tests and those of the remedy fuel rod tests. The effects of cooling conditions on RIA fuel behavior are discussed in section 2 based on subcooling parameter tests, flow shroud tests, bundled rod tests and forced coolant flow tests. In section 3 are summarized the test results with BWR remedy fuel rods. RIA fuel behavior of zirconium-lined and cupper-barrier cladding rods are compared with those of conventional zircloy-2 cladding reference rods.

2. Effects of Cooling Conditions

2.1 Coolant Subcooling

All the NSRR tests were performed under ambient temperature conditions. Consequently, fuel rods were cooled quite effectively by highly subcooled coolant. In the first step of examining the effects of cooling conditions on RIA fuel behavior, coolant subcooling was changed from room temperature to 90°C. Water temperature in the test capsule was raised to a predetermined temperature by an electric heater under ambient pressure, then RIA transient was initiated while keeping the coolant temperature constant.

Figure 1 shows a comparison of typical cladding temperature histories for different coolant temperatures at the energy deposition of 180 cal/gUO_2. As the coolant temperature was elevated, both the maximum cladding temperature and the duration of film boiling was increased. Figure 2 is a data plot of maximum cladding temperatures, quenching temperatures and film boiling duration periods as a function of coolant subcooling. This plotting indicates that the decrease of subcooling affects in two ways to the cladding thermal behavior; one is to decrease the heat transfer coefficient during film boiling regime resulting in higher cladding temperature attained for the same fuel enthalpy rise, and the other is to decrease the temperature at quenching initiation. A significant increase of film boiling duration period was resulted by the duplication of these two kinds of influences.

In Figure 3 the maximum cladding temperatures under low subcooling (T_{sub} = 10°C) are compared with those of standard tests (T_{sub} = 75°C) as a function of energy deposition. The maximum temperatures at a given energy deposition for lower subcooling are by 300 to 500°C higher than those for the higher subcooling cases for the test range of 180 to 240 cal/gUO_2. The plot also exhibits that the fuel failure occurred when the maximum temperature measured at cladding surface exceeded about 1800°C for both the low and high subcooling cases. Consequently, it will be concluded that the threshold energy for rod failure decreased about 50 cal/gUO_2 by cooling capability reduction when coolant subcooling was decreased from 75°C to 10°C.

The influence of coolant subcooling on fuel failure behavior are summarized in Figure 4 as a data plot of energy deposition versus coolant temperatures. Energy deposition necessary for fuel fragmentation as well as for failure initiation decreased apparently as the coolant subcooling is decreased.

2.2 Flow Shroud and Fuel Rod Clusters

Areal ratio of coolant to fuel is another important cooling environmental condition. Coolant to fuel ratio of actual reactor core was simulated by attaching a flow shroud to a single rod, or by assembling a small rod cluster. Four types of flow shroud, as shown in Figure 5, were used to examine the effects of the size and shape of the shroud. In cluster tests, five rod cluster, comprised of a 20% enriched center fuel rod surrounded by four 10% enriched outer fuel rods, was used.

Cladding surface temperature histories at different elevations of a rod in a flow shroud are compared in Figure 6. During first 6 seconds after the transient, no evident differences are observed among the temperature curves. The histories in the standard tests, without-flow-shroud cases, are nearly the same during this initial period. After 6 seconds, however, in with-flow-shroud cases, film boiling is sustained extending to 20 seconds at the highest measuring point.
It is understood that the effect of flow shroud was not evident

during the first several seconds because the natural convection was not effectively developed and the vapor film was still quite thin when compared with the water gap thickness. Maximum cladding temperatures were, consequently, not strongly influenced by the flow shroud. The effect of the shroud appears in cooling down period after the natural convection in the shroud is established. Coolant subcooling must be reduced in downstream and steam binding may possibly have ocurred in large energy deposition cases. Figure 7 shows a comparison of the data from subcooling parameter tests and those from flow shroud tests regarding the quenching temperature and the time to quench respectively. A good agreement of flow shroud test data with the data from subcooling parameter test will prove that the extension of film boiling duration was mainly caused by reduced subcooling.

Figure 8 summarizes the tendency of cladding thermal behaviors as a function of water to fuel areal ratio. Maximum cladding temperature was not influenced by the shroud as discussed above. Larger decrease of quenching temperature and increase of film boiling duration was resulted for smaller water to fuel ratio.

In Figure 9, failure behavior of shrouded rods is illustrated. Fuel failure threshold decreased about 30 cal/gUO_2 for shrouded rods. Longer duration of film boiling may mainly be responsible for this decrease.

The rod clusters showed similar behavior as shrouded rods. In Figure 10, cladding temperature history of a center rod in a five rod cluster is compared with that of a single rod test at around 230 cal/gCO_2. Extended film boiling duration and higher temperatures during cooling down period are observed as in the case of shrouded rod tests. Comparatively large temperature recovery from 4 to 11 seconds at No. 1 thermocouple position which faced to the outer rod may be caused by the hot wall effect of the outer rod. Local steam binding and the additional heating by the outer rod are imagined to have occurred at this narrow coolant space. There exists a little difference in maximum temperatures. This difference was mainly

caused by the variation of energy deposition. Another peculiar phenomena in the rod cluster tests is a largely eccentric distribution of energy deposition in the outer rods. Figure 11 is a relative energy distribution in the five rod cluster calculated by a two dimensional diffusion code. This skew of energy deposition resulted in a large difference of cladding temperature between inner and outer side of an outer rod under rapid heating up of an RIA.

2.3 Forced Coolant Flow

RIA fuel behavior tests under forced coolant flow conditions will be started shortly in NSRR in-pile loop facility. In order to get preliminary information for the loop experiment, a coolant circulation circuit was assembled in a standard test capsule and the effects of coolant flow were examined.

Figure 12 shows a schematic of the test assembly. The water in the capsule was circulated by a small immersion pump and the flow rate was measured by a drag-disc type prompt response flowmeter.

Cladding temperature histories for different coolant flow conditions are compared in Figure 13. Remarkable decrease of maximum cladding temperature and duration of film boilding can be noted. Maximum cladding temperatures, quenching temperatures and film boiling duration periods are plotted as a function of coolant velocity in Figure 14. The effects of coolant flow on fuel thermal behaviors, i.e. the rate of decrease of cladding temperature and film boiling duration for coolant flow, are very large for lower flow velocities, and tend to saturate at higher velocities.

2.4 Conclusion

The effect of cooling conditions on RIA fuel behavior will be summarized as follows.

(1) Thermal behavior

(a) Decrease of coolant subcooling caused lower heat transfer coefficient and lower quenching temperature at cladding surface. These effects resulted in higher maximum cladding

temperature and longer film boiling duration.

(b) Restriction of the amount of coolant water in the flow shroud affected the fuel behavior during the cooling down period after natural convection was established. Therefore, the maximum cladding temperature was not strongly influenced by flow shroud, while the film boiling duration was extended to 10∿20 seconds.

(c) In bundled rod tests the restriction of the coolant inventory was the major effect on fuel thermal behavior. Extension of film boiling was observed as was in the with-flow-shroud tests. Additionally, local overheating was observed at cladding surface faced to the narrowest coolant gap.

(d) Forced coolant flow promoted the film boiling heat transfer at cladding surface significantly. Large decrease of cladding temperature and film boiling duration was observed.

(2) Failure Threshold

(a) Higher cladding temperature and longer film boiling duration caused by the decrease of coolant subcooling or by the restriction of the amount of coolant water resulted in the decrease of failure threshold by 20 to 50 cal/gUO_2.

(b) Enhanced cooling capability by forced coolant flow resulted in the increase of failure threshold by around 30 cal/gUO_2 under ambient coolant temperature and pressure conditions.

3. Results of Remedy Fuel Rod Tests

RIA fuel behaviors of remedy fuel rods were studied in NSRR. Three types of BWR fuel rods, currently used GE reference rods, zirconium-lined and cupper-barrier cladding rods, were compared in this test series. Major characteristics of the test rods are listed in Table 2.

Total of 17 rods were irradiated so far under ambient coolant temperature and pressure conditions, and the effects

of the zirconium lining and the cupper barrier under power burst condition of RIAs were examined by comparing with the results with current design reference rods. The energy deposition applied and the failure occurrences are summarized in Figure 15. The failure threshold energy for any type of BWR rods tested was 260 to 280 cal/gUO_2 which is equal to or a little higher than that for NSRR standard rods. A single exception is that a zirconium-lined rod did not fail at 300 cal/gUO_2 which is about 40 cal/gUO_2 in excess of the failure threshold.

Photographs of post irradiated rods are shown in Figure 16. In general, extent of damage by appearance was rather milder in the BWR rods than in NSRR standard rods. This may probablly have been resulted from the larger cladding thickness which secured higher rigidity of the cladding during RIA transient. In the NSRR tests with thinner cladding rods in which cladding thickness was reduced to about 65% of the standard, failure threshold decrease of about 50 cal/gUO_2 and more intensive damage to the rod were observed.

Maximum cladding temperatures of GE reference and remedy fuel rods compared with the data from NSRR standard tests in Figure 17. The temperatures of GE rods were generally a little lower than those of NSRR standard cases for the energy deposition range tested. The milder damage of BWR rods will be influenced by this tendency of clad temperature, too.

When compared among the GE rods, the temperatures of cupper-barrier rods were higher than those of other GE rods at lower energy depositions. This difference of cladding temperatures suggests that the melted cupper on the inner surface of the cladding may have acted as a thermal bond promoting the gap heat transfer during the contact phase of the transient. It is reasonable that this effect disappeared at higher energy depositions, because the zircaloy base reached metling temperature promptly at the energy of near failure threshold.

Conclusions of the remedy fuel rod tests can be summarized as follows:

(1) Failure threshold energy of BWR rods is equal to or a little higher than that of NSRR standard rods.

(2) Zirconium-lining had no influences on thermal behavior, nor failure threshold energy.

(3) Cupper-barrier caused to higher cladding temperatures at lower energy depositions, but had no evident influences on failure threshold.

Reference

1. M. Ishikawa; First Progress Report of the Nuclear Safety Research Reactor (NSRR) Experiments 4th LWR Safety Information Meeting, Washington(Sept, 1976)
2. M. Ishikawa, et al., "Some Experience and Plans on Reactor Safety Research by NSRR" 1st US/Japan Seminar on Fast Pulse Reactors Tokai, Japan (1976)
3. S. Saito, T. Fujishiro, T. Inabe, M. Ishikawa; "Some Experiences and Inpile Experimental Programme on Fuel Coolant Interaction in NSRR", 3rd Specialist Meeting on Sodium/Fuel Coolant Interaction in Fast Reactors, in Tokyo, Japan (1976)
4. M. Ishikawa; "Study on Fuel Behavior under Reactivity Initiated Accident Condition", Journal of the Thermal and Nuclear Power Vol 28, No 5 (1976)
5. M. Ishikawa, T. Fujishiro, T. Inabe, K. Iwata: NSRR Experiments on LWR Fuel Behavior under Reactivity Accident Conditions, American Nuclear Society Topical Meeting, Thermal Reactor Safety, Sun Valley (July, 1977)
6. A. Morishima, M. Ishikawa, S. Suguri : Safety of Light-Water Reactor Fuel, IAEC-CN-361549, "Nuclear Power and Its Fuel Cycle "Vol 2, IAEA, Vienna (1977)
7. M. Ishikawa, T. Hoshi, N. Onishi, T. Yoshimura; Progress Report on NSRR Experiments, (1) - LWR Fuel Failure under Reactivity Initiated Accident Condition in Ambient Temperature and Pressure Coolant, Journal of the Atomic Energy Socity of Japan, Vol.19, 17(1977)
8. M. Nozawa, M. Ishikawa, S. Saito: Fast Reactor Fuel Test Program in the NSRR, NRC/RSR-Japan FBR Safety Research and Development Meeting Tokyo,(Nov. 1978)
9. S. Suguri, M. Ishikawa, S. Saito, Results of Inpile Experiments in the NSRR on Reactivity Initiated Accidents, Projekt Nuklear Sicherheit Jahreskolloquim, (1978)
10. T. Hoshi et al; Fuel Failure Behavior of Unirradiated Fuel Rods under Reactivity Initiated Accident Conditions, Journal of Atomic Energy Society of Japan, Vol. 20 No.9 (1978) in Japanese
11. M. Ishikawa, T. Hoshi, N. Ohishi, S. Saito, T. Yoshimura; Progress Report on NSRR Experiments, (II)-LWR Fuel failure under Reactivity Initiated Accident Condition in Ambient Temperature and Pressure Coolant, Journal of the Atomic Energy Society of Japan, Vol. 20, No. 10 (1978)
12. S. Kobayashi, N. Ohnishi, T. Yoshimura, W.G.Lussie; Experiment Results of Some Cluster Tests in NSRR, Journal of the Atomic Energy Society of Japan, Vol.15, No. 6 (1978)
13. T. Fujishiro, T. Hoshi, S. Yanagihara, M. Ishikawa; A Study on Pressure Generation Caused by Actual Fuel Failure in the NSRR Experiment, Fourth CSNI Specialist Meeting on Fuel-Coolant Interaction in Nuclear Reactor Safety, Bourmemouth (April 1979)
14. M. Ishikawa, T. Inabe; The Nuclear Safety Research Reactor (NSRR) in Japan, Advances in Nuclear Science and Technology, Vol.11, Plenum Press, New York, 1979

21. M. Ishikawa and K. Tomii(ed): Quarterly Progress Report on the NSRR Experiments (1); Combined, October 1975 - March 1976, JAERI - M 6635 (June, 1976)

22. M. Ishikawa and K. Tomii(ed): Quarterly Progress Report on the NSRR Experiments (2); Combined, April 1976 - June 1976, JAERI - M 6790 (October, 1976)

23. M. Ishikawa and K. Tomii(ed): Quarterly Progress Report on the NSRR Experiments (3); Combined July 1976 - December 1976, JAERI - M 7051 (March, 1977)

24. Reactivity Accident Laboratory and NSRR Operation Section: Quarterly Progress Report on the NSRR Experiments (4); Combined, January 1977 - June 1977, JAERI-M 7304 (August, 1977)

25. Reactivity Accident Laboratory and NSRR Operation Section: Quarterly Progress Report on the NSRR Experiments (5); Combined, June 1977 - December 1977, JAERI-M 7554 (January, 1978)

26. Reactivity Accident Laboratory and NSRR Operation Section: Quarterly Progress Report on the NSRR Experiments (6); Combined, January 1978 - June 1978, JAERI-M 7977 (October, 1978)

27. Reactivity Accident Laboratory and NSRR Operation Section: Semiannual Progress Report on the NSRR Experiments (7); Combined, July 1978 - December 1978, JAERI-M 8259 (May, 1979)

Table 1 Number of NSRR Experiments (Oct.'75 - June'79)

Test Items	Number of Tests		
	Oct.'75 - Mar.'78	Apr.'78 - June'79	Total
1. Standard Fuel Tests			
Scoping tests	46	2	48
Fuel centerline temperature measurements	3	0	3
Fuel enlongation measurements	3	10	13
2. Fuel Design Variation Tests			
Gap width parameter tests	13	3	16
Gap gas parameter tests	3	7	10
Enrichment tests	17	0	17
Pre-pressureized fuel tests	29	8	37
Specially heat-treated zircaloy cladding tests	5	8	13
SUS cladding tests	6	3	9
3, Cooling Environmental Variation Tests			
Coolant temperature parameter tests	10	7	17
Flow area simulation tests	20	2	22
Forced circulation tests	0	9	9
Bundled fuel tests	8	2	10
4. Defective Fuel Tests			
Waterlogged fuel tests	46	13	59
Fretting corroded fuel tests	11	1	12
5. NRC-GE Fuel Tests	0	17	17
6. Miscellaneous Tests	20	26	46
7. High Pressure Capsule Tests	0	2	2
Total	240	120	360

Table 2 Characteristics of GE Fuel Rods

Type of fuel rods tested	
CC	GE reference fuel rod
DC 1	Zr lined fuel rod
DC 2	Cu barrier fuel rod
Cladding material	Zr-2
Fuel pellets	
Enrichment	10% U-235
Density	95% T.D.
Geometry	
Dimension	
Pellet O.D.	10.57 mm
Cladding O.D.	12.52 mm
Cladding wall thickness	0.86 mm
Gap width	0.115 mm
Zr-liner thickness	~10% of wall thickness
Cu-barrier thickness	~0.01 mm

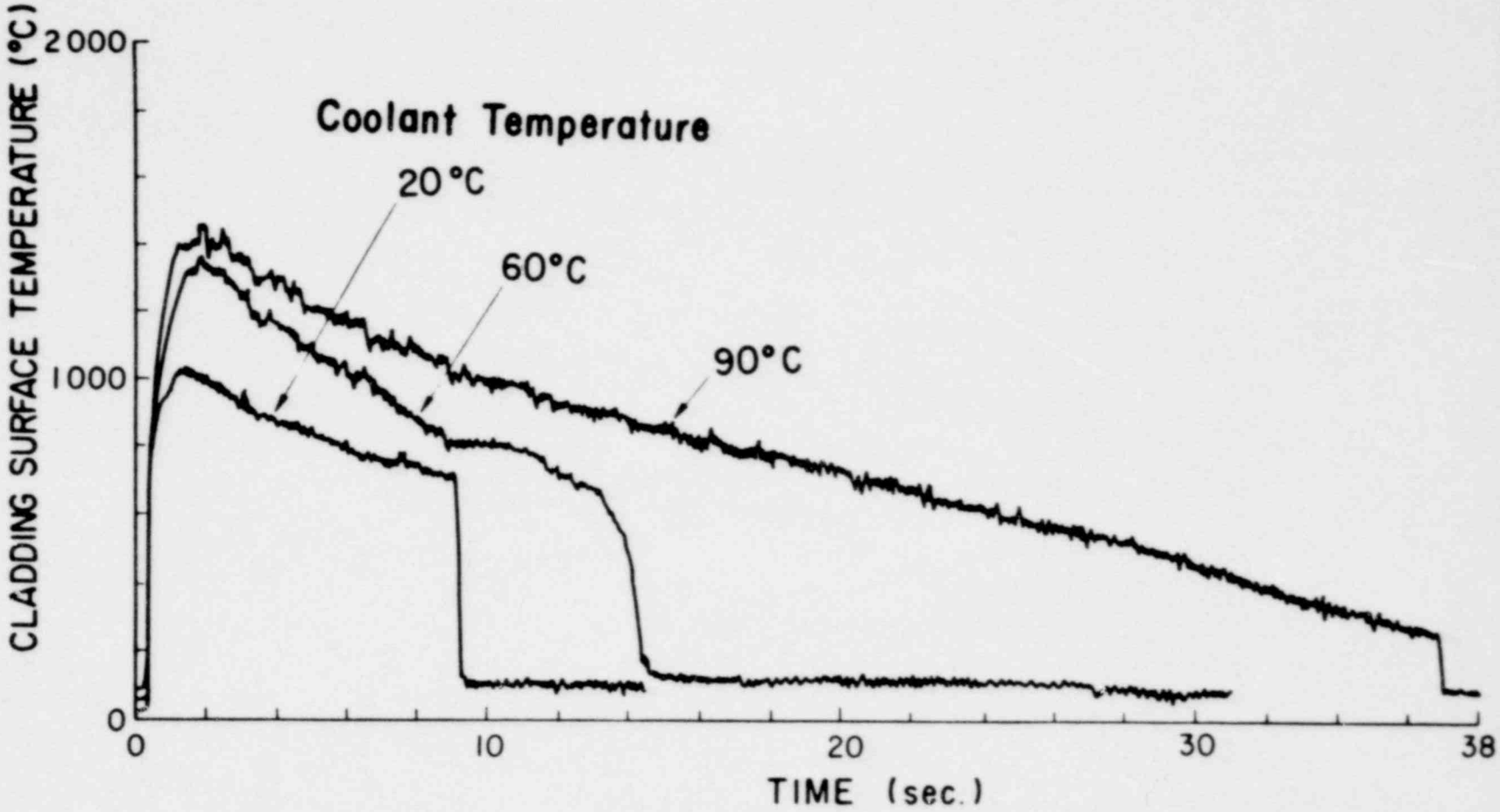

Fig.1 Comparison of Cladding Surface Temperature Behaviors for Different Coolant Temperatures.

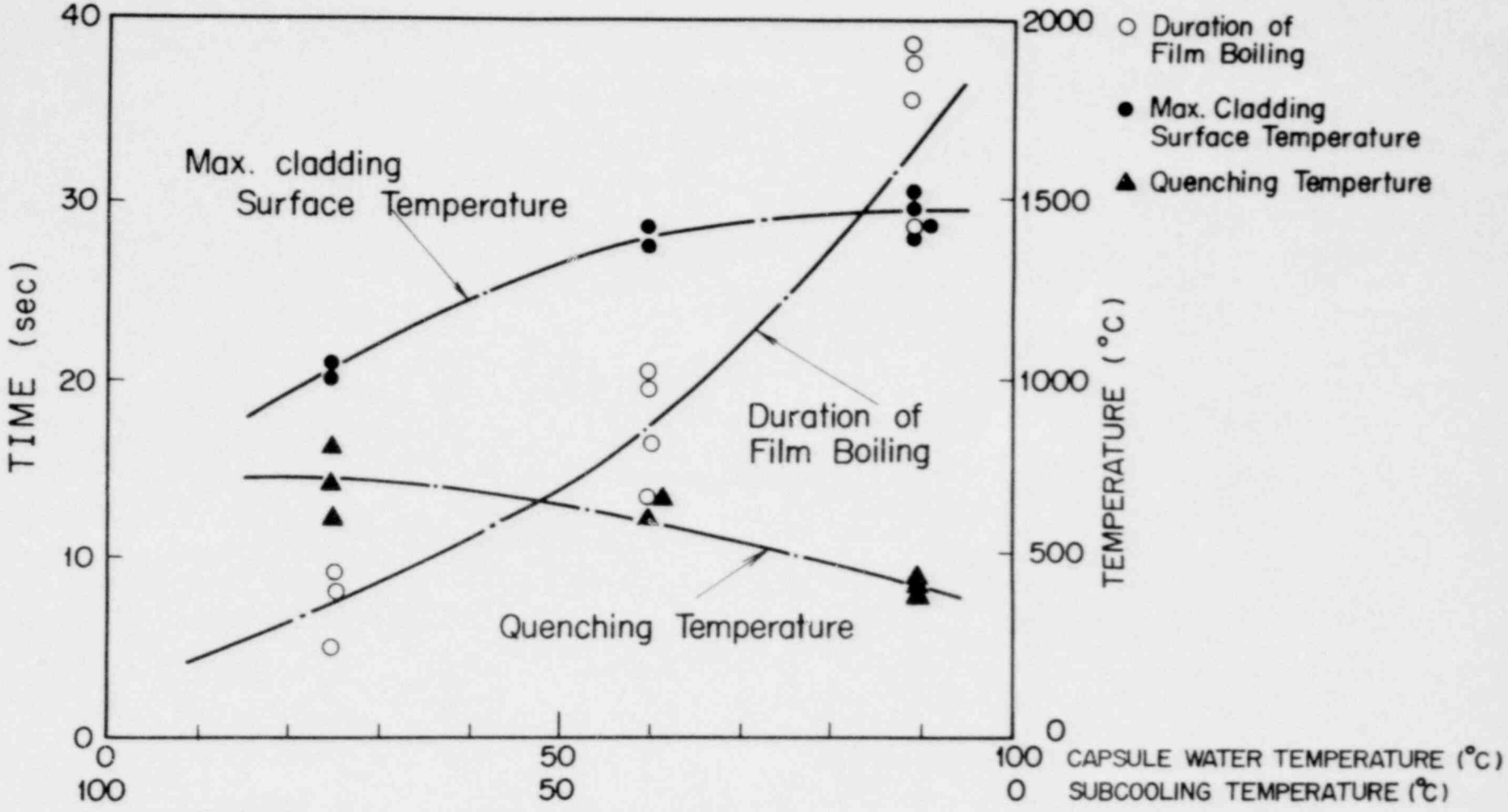

Fig. 2 The effect of coolant subcooling on maximum cladding temperature, quenching temperature and duration of film boiling (180 cal/g·UO_2)

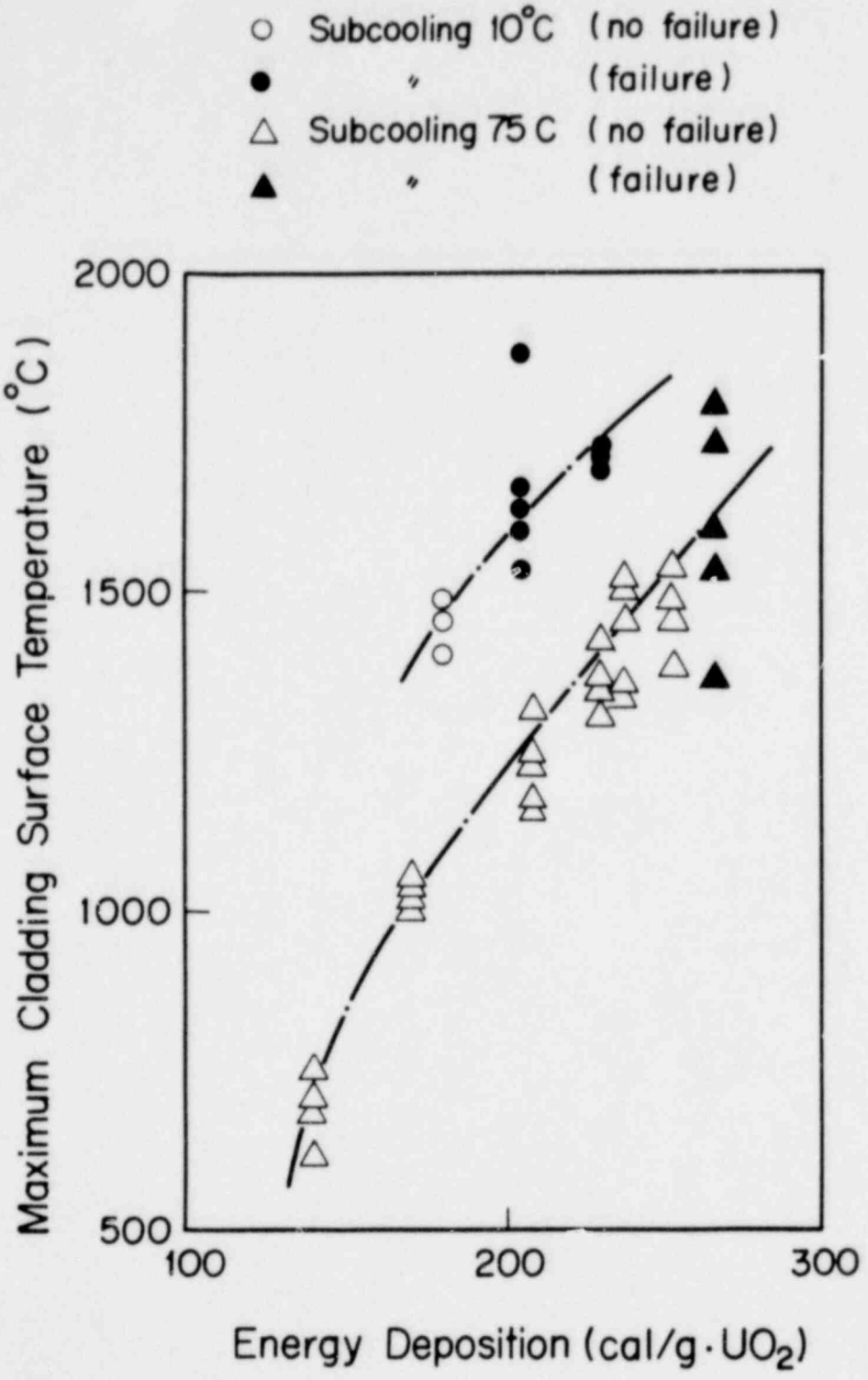

Fig. 3 Maximum cladding surface temperatures as a function of energy deposition

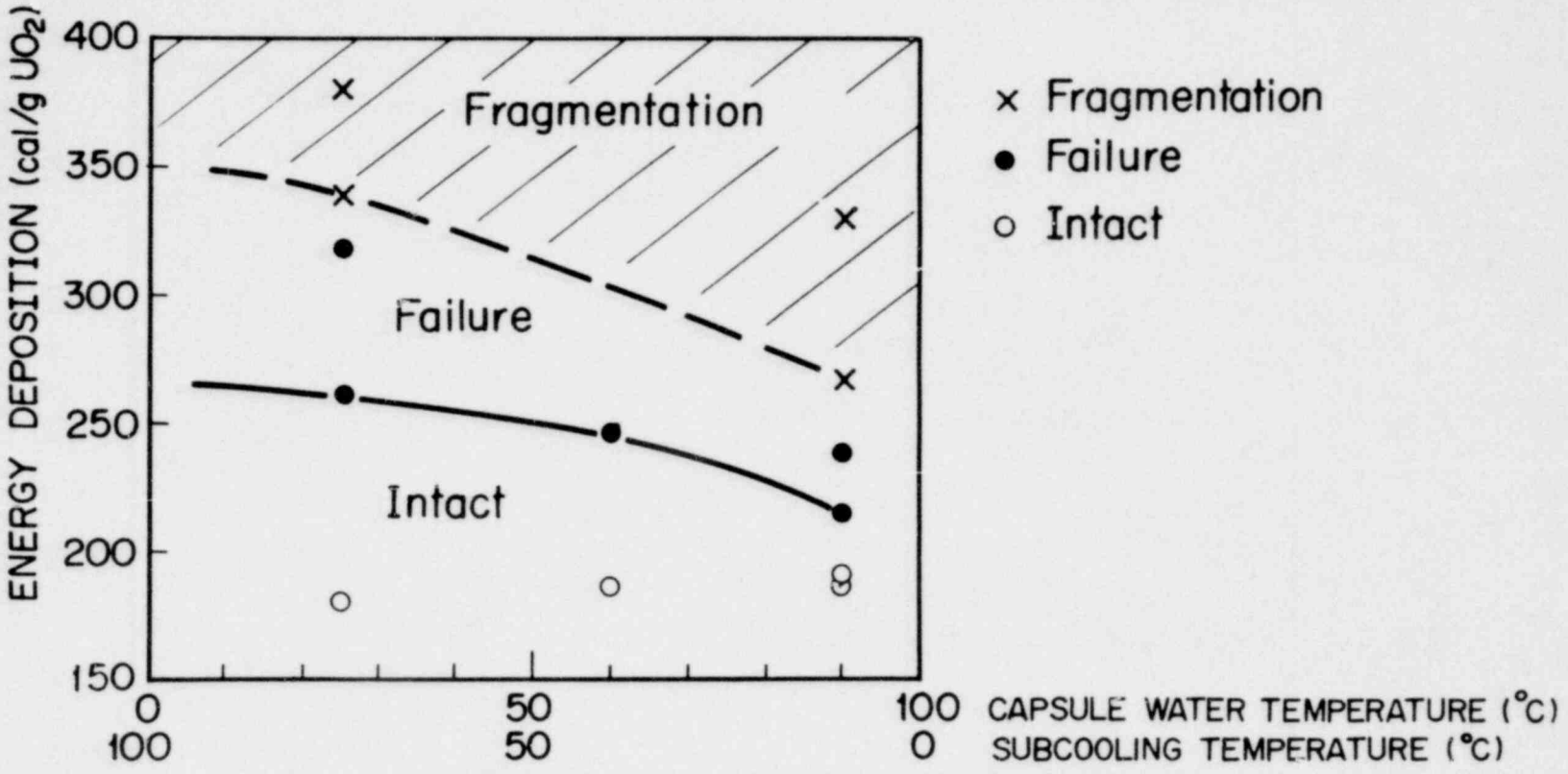

Fig.4 Threshold energy depositions for fuel failure and fragmentation as a function of coolant subcooling

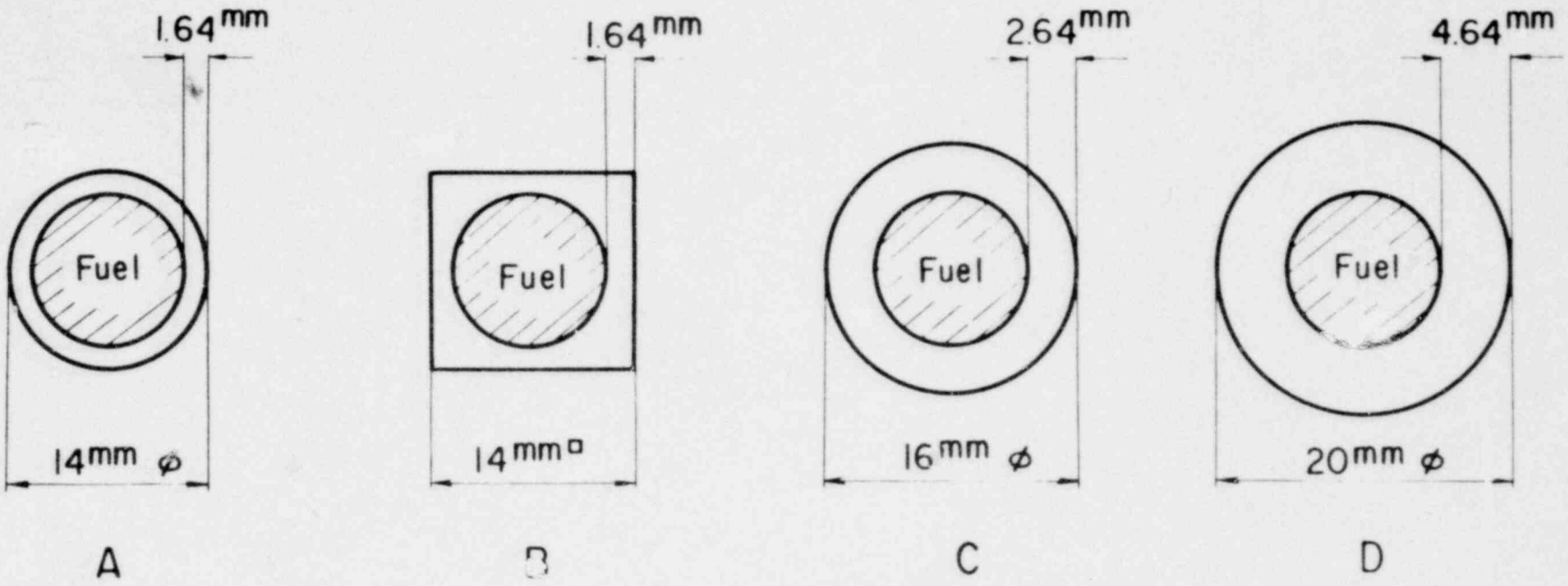

Fig. 5 Cross Section of Flow Shrouds

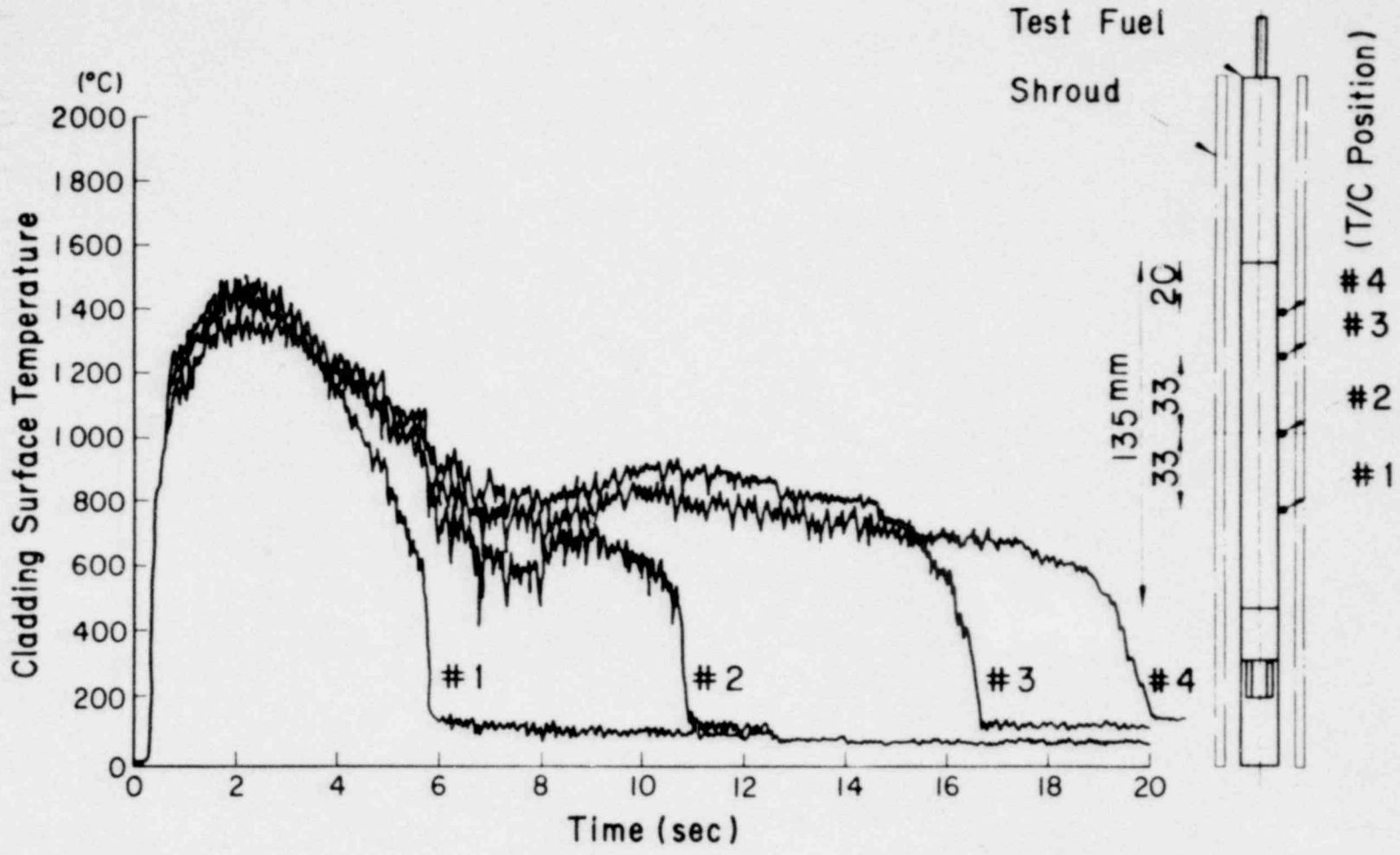

Fig. 6 **Histories of the Cladding Surface Temperatures in Test No. 233-6 (211 cal/g·UO_2).**

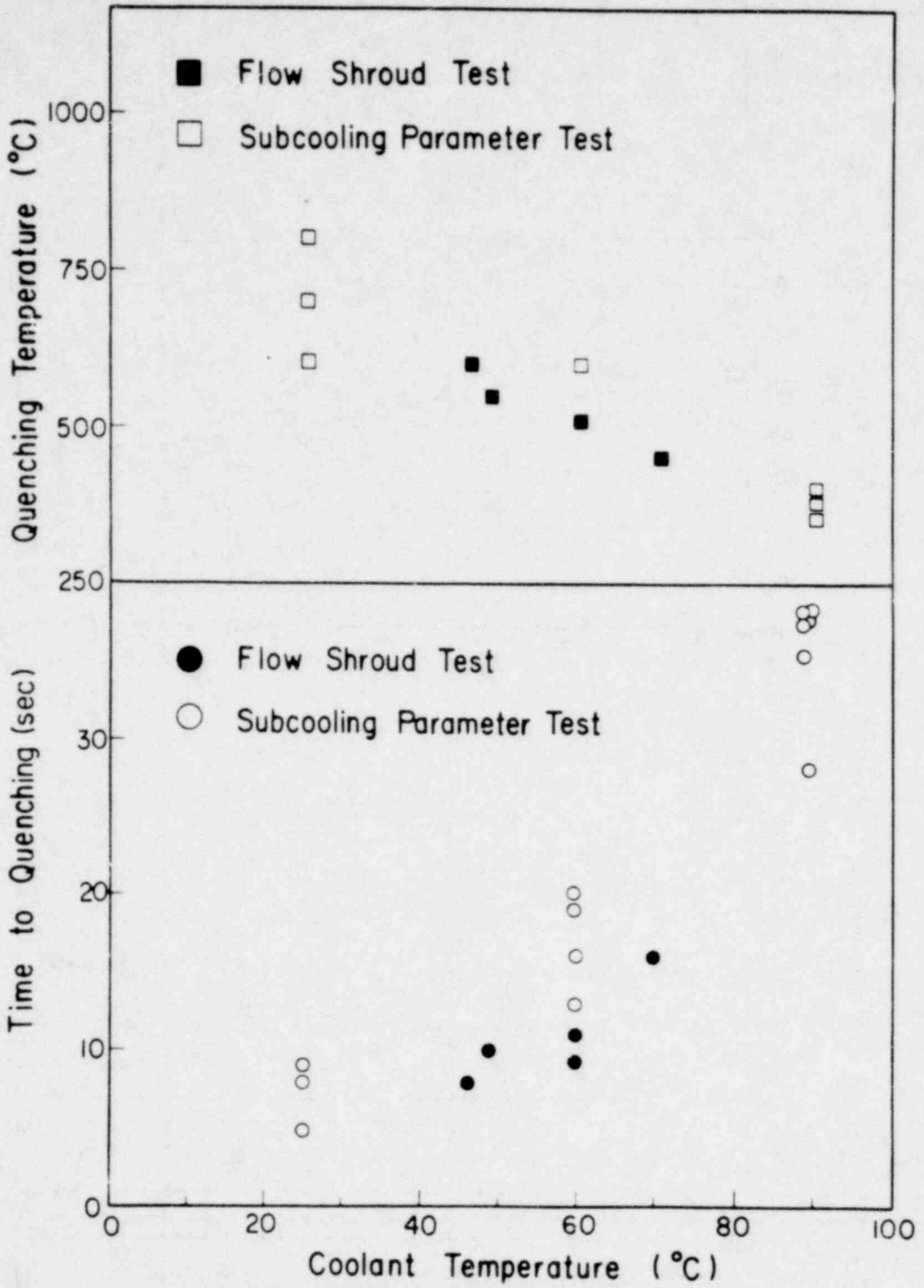

Fig.7 Quenching Temperatures and Time to Quenching in Flow Shroud Tests and Subcooling Parameter Tests

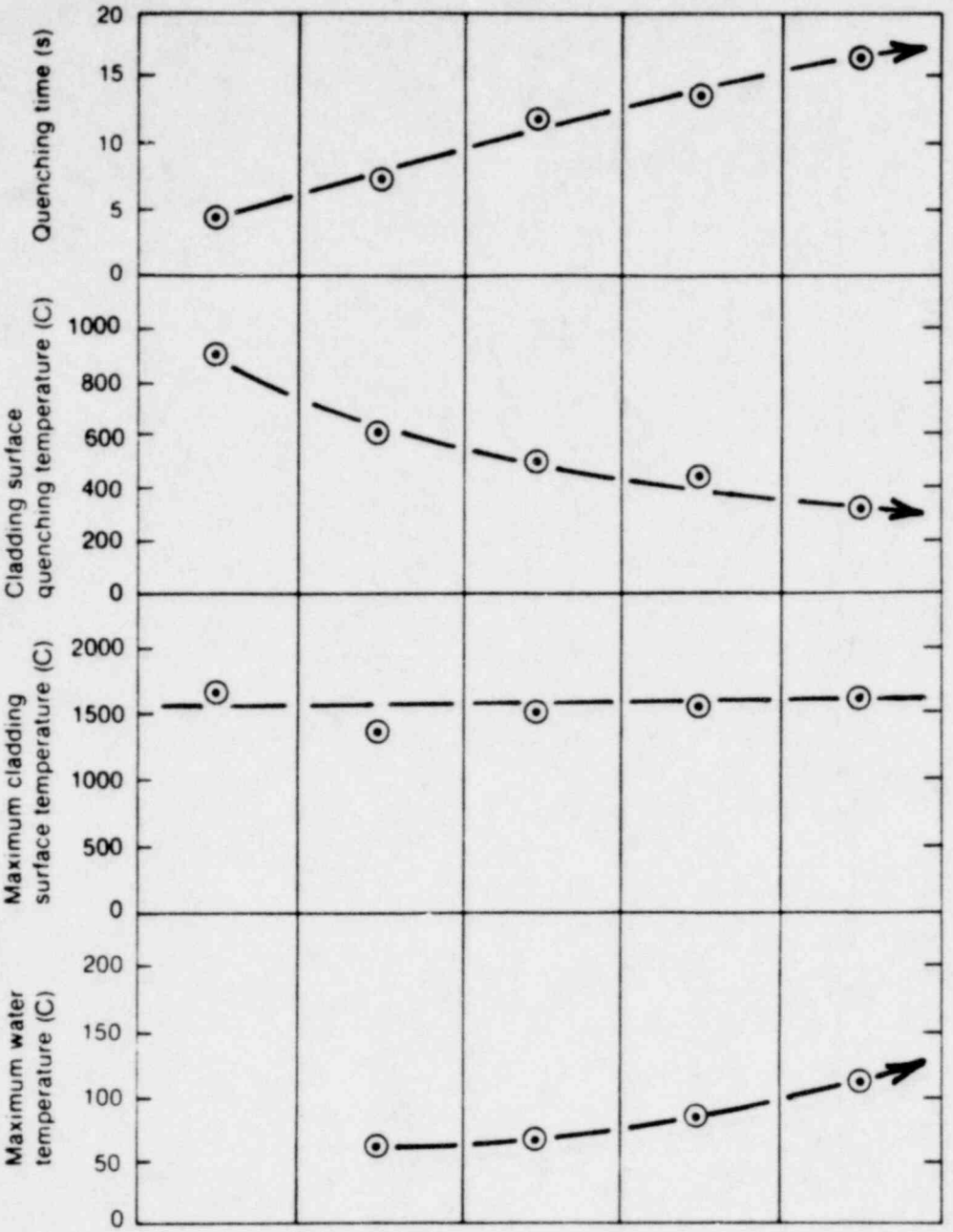

Total radial average energy deposition (cal/g UO_2)	250	240	237	251	247
Shroud	None	20-mm cyl	16-mm cyl	14-mm sq	14-mm cyl
Water/fuel ratio	250	2.48	1.23	1.20	0.71

Fig.8 Temperature related behavior as a function of water to fuel areal ratio

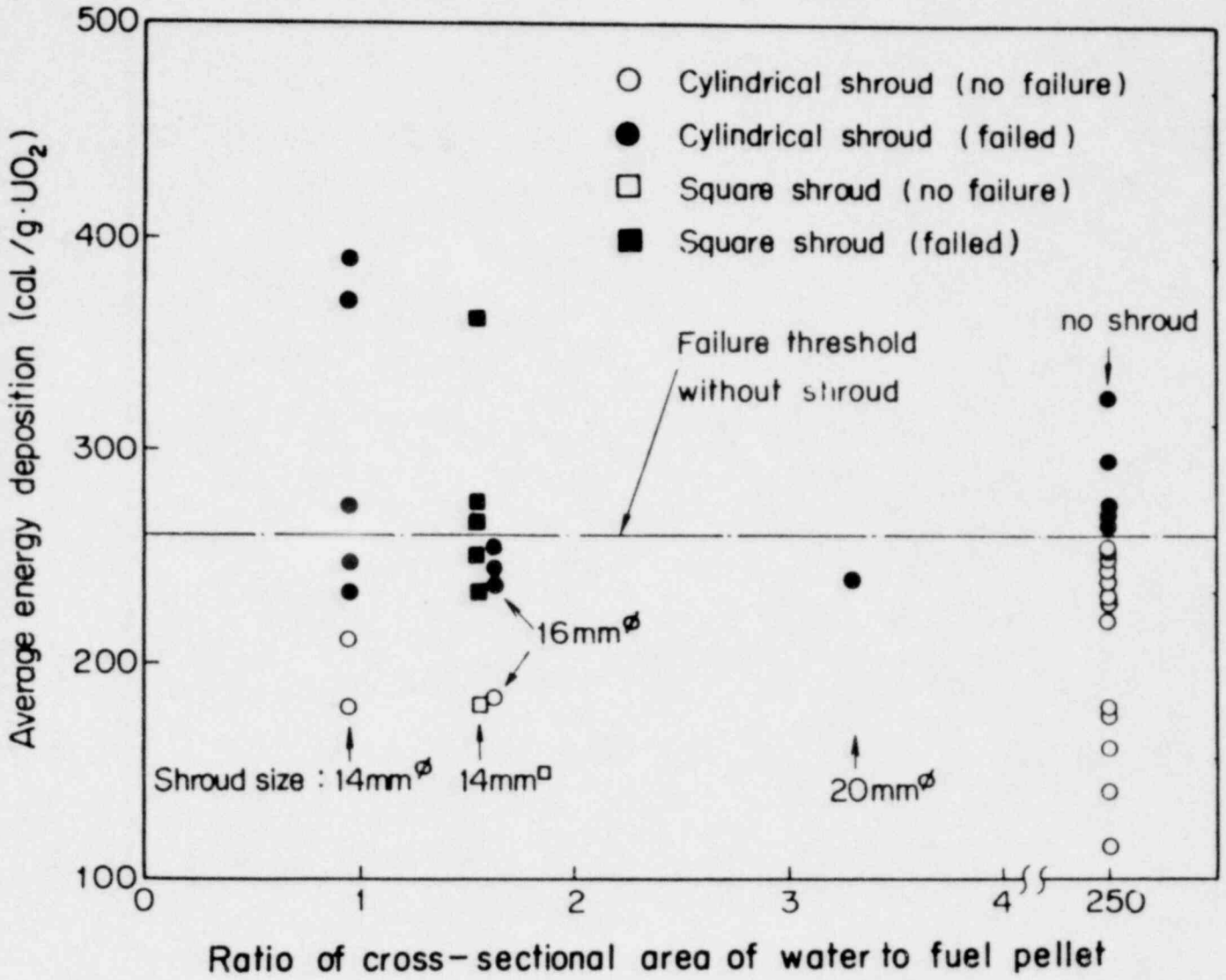

Fig.9 Failure behavior of shrouded rods as a function of water to fuel areal ratio

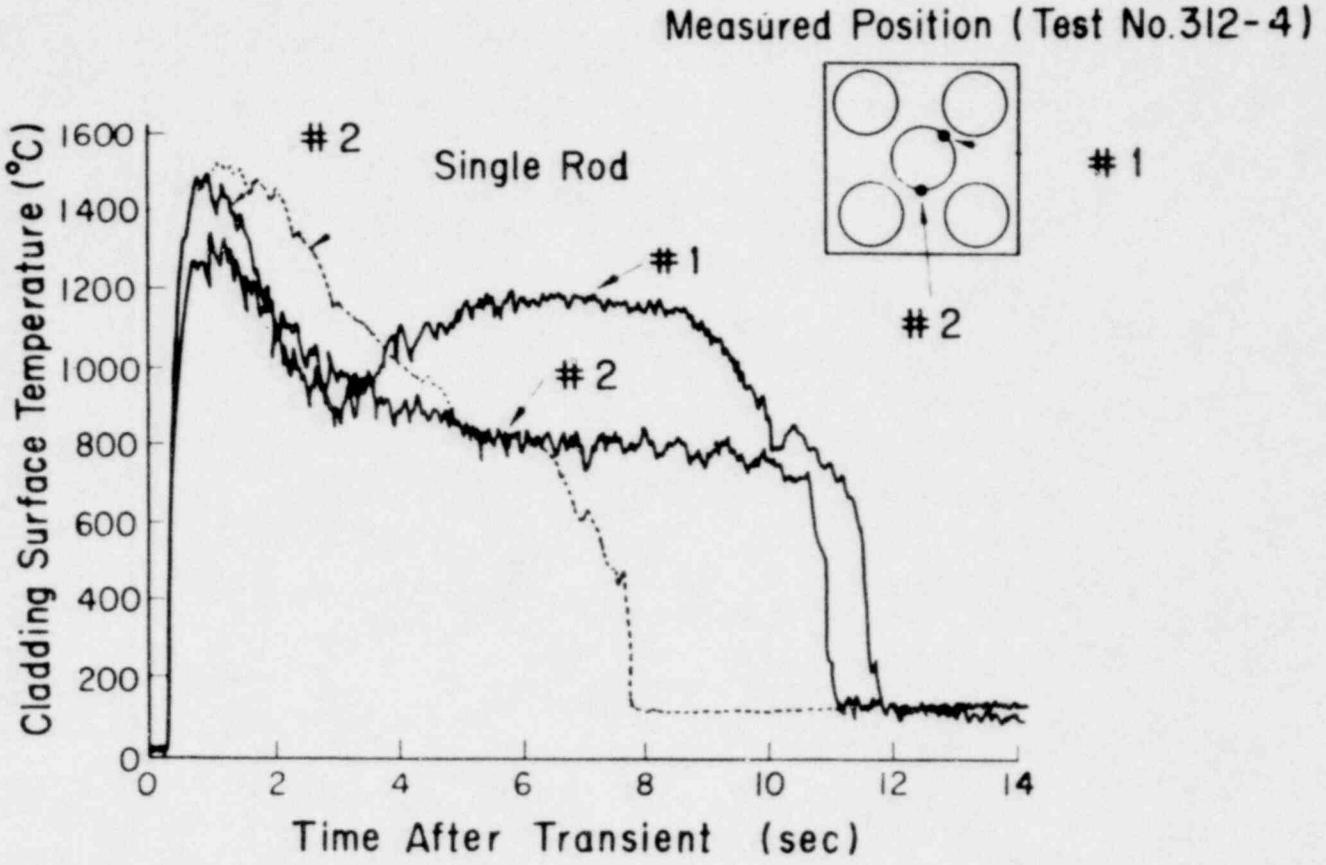

Fig.10 Cladding Surface Temperature Histories at Active Fuel Length Center During Bundle Rod Test No. 312-4 (214 cal/g·UO_2) and Single Rod Test with 20% E. Fuel, Test No.221-6 (232 cal/g·UO_2).

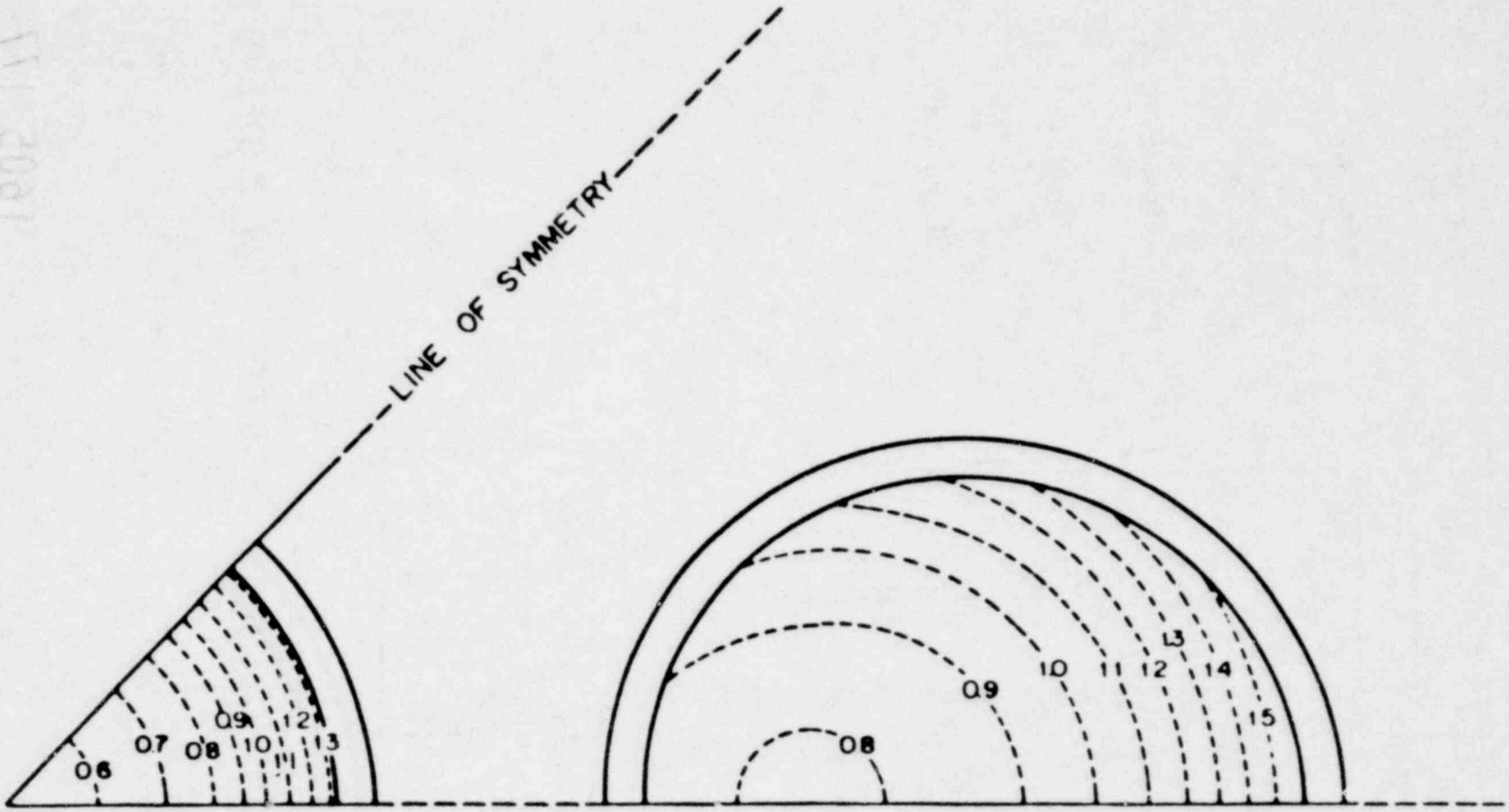

Fig. 11 **Relative Energy Distribution in the Five Rod Clusters.**

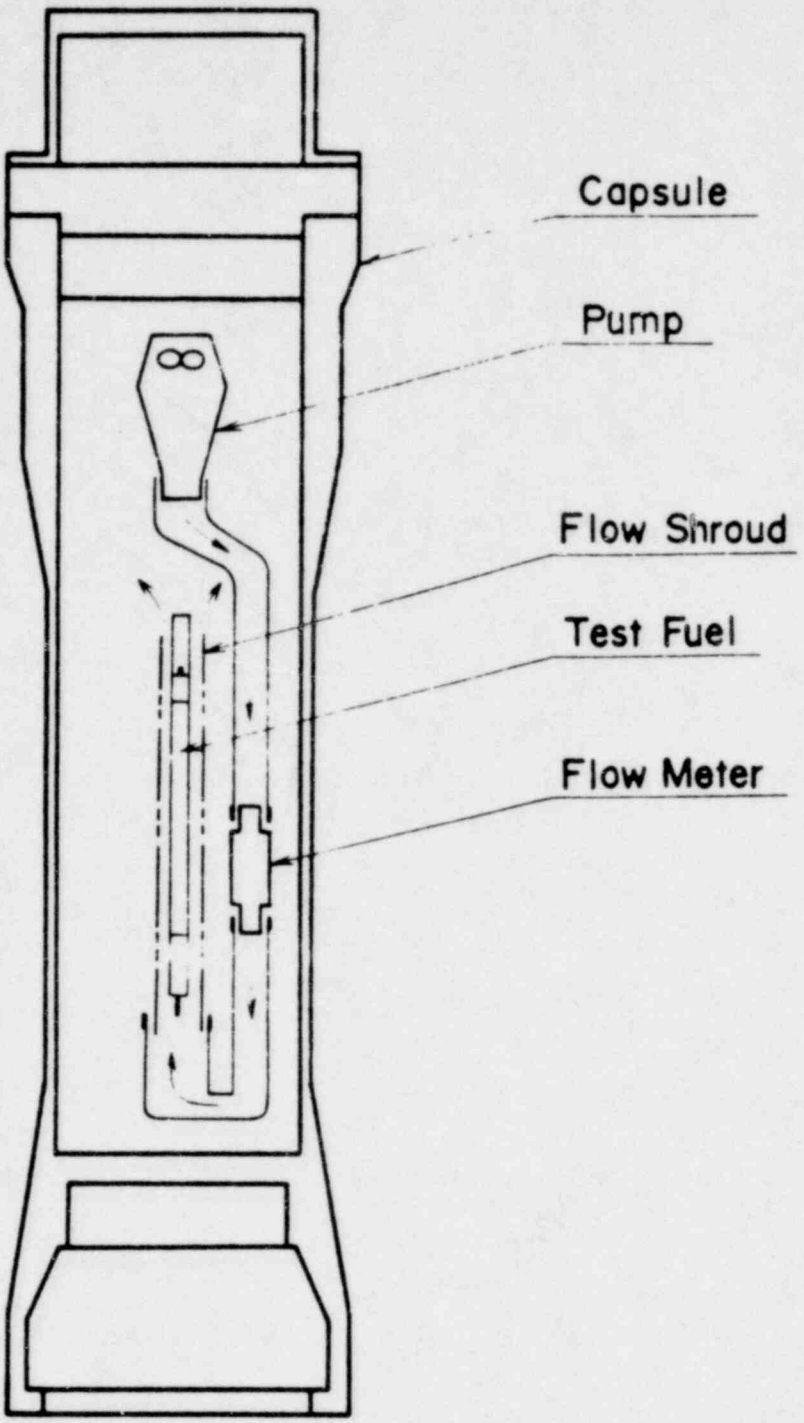

Fig. 12 Schematic of forced coolant flow experiment

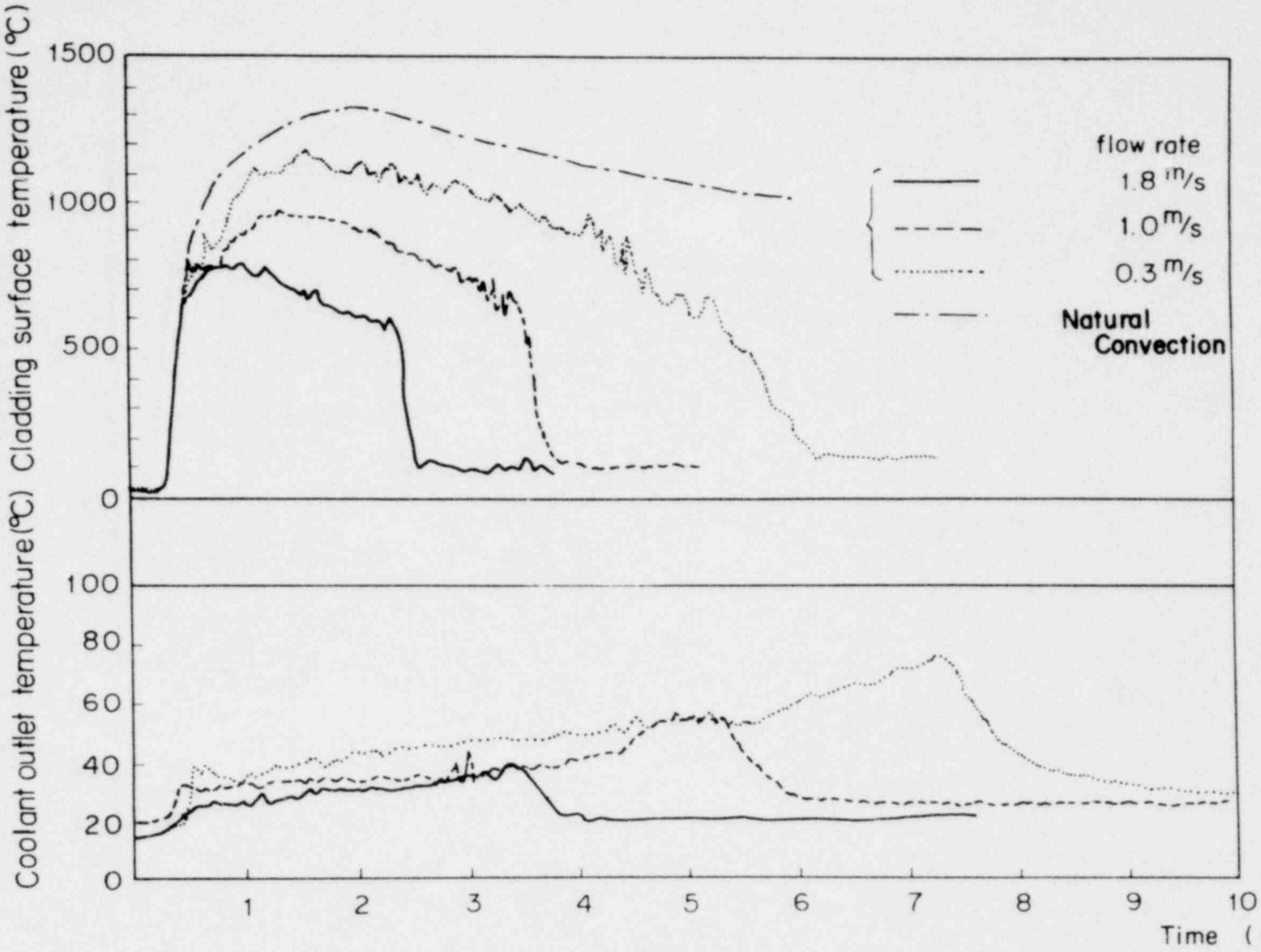

Fig. 13 Transient Histories of Cladding Surface Temperatures and Coolant Outlet Temperatures at 190 $cal/g \cdot UO_2$

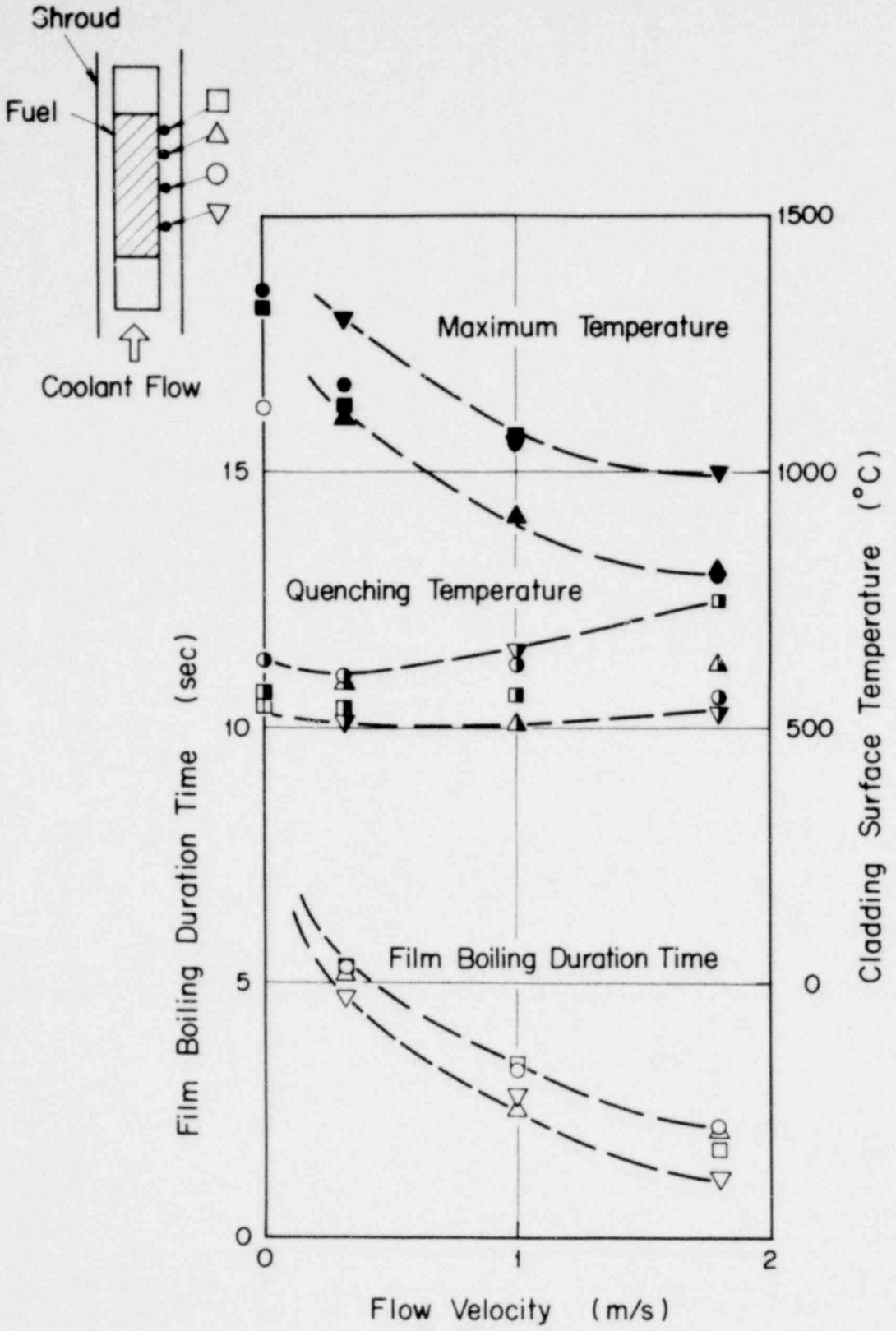

Fig. 14 Effect of coolant velocity on maximum cladding temperature quenching temperature, and film boiling duration time at 190 cal/g UO_2

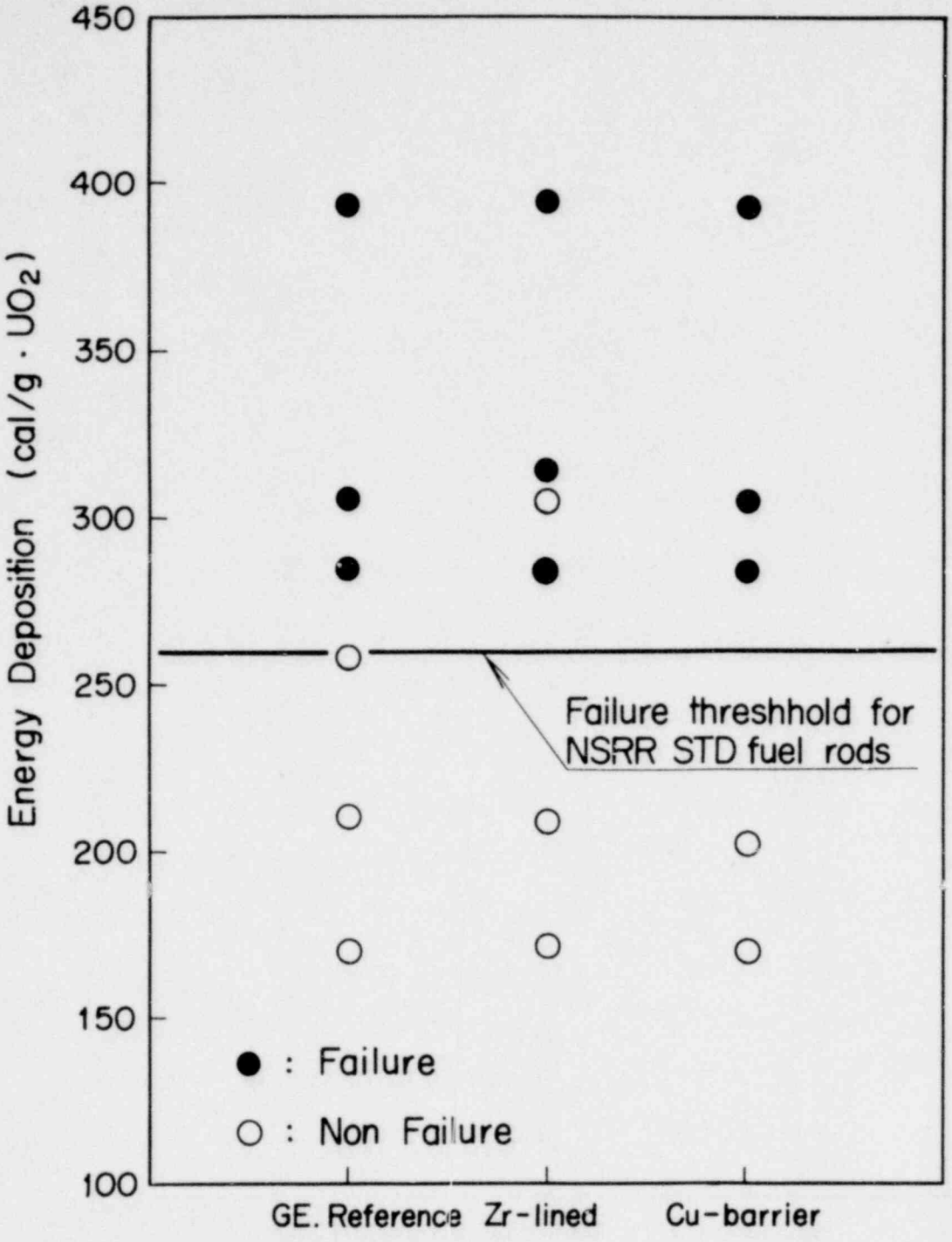

Fig. 15 Comparison of failure threshold for GE fuel rods

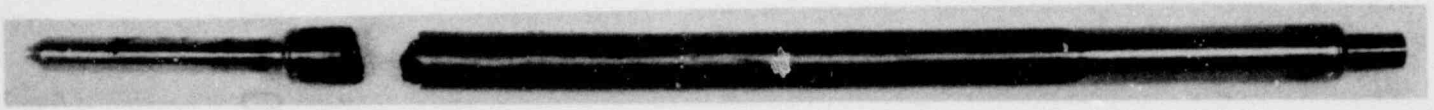

Ge-reference rod
(Test No, 501-7)

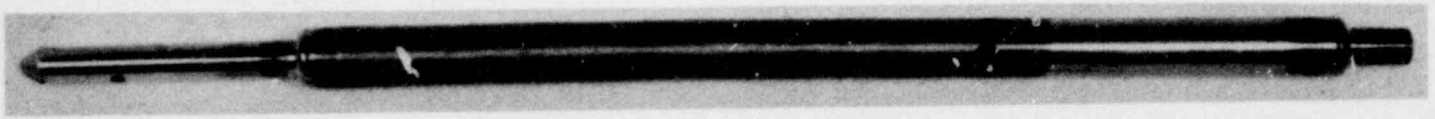

Zirconium-lined Cladding rod
(Test No. 502-4)

Cupper-barrier Cladding rod
(Test No. 503-4)

Fig. 16 Post test photographs of GE-reference and remedy fuel rods irradiated at 305 cal/g.UO_2

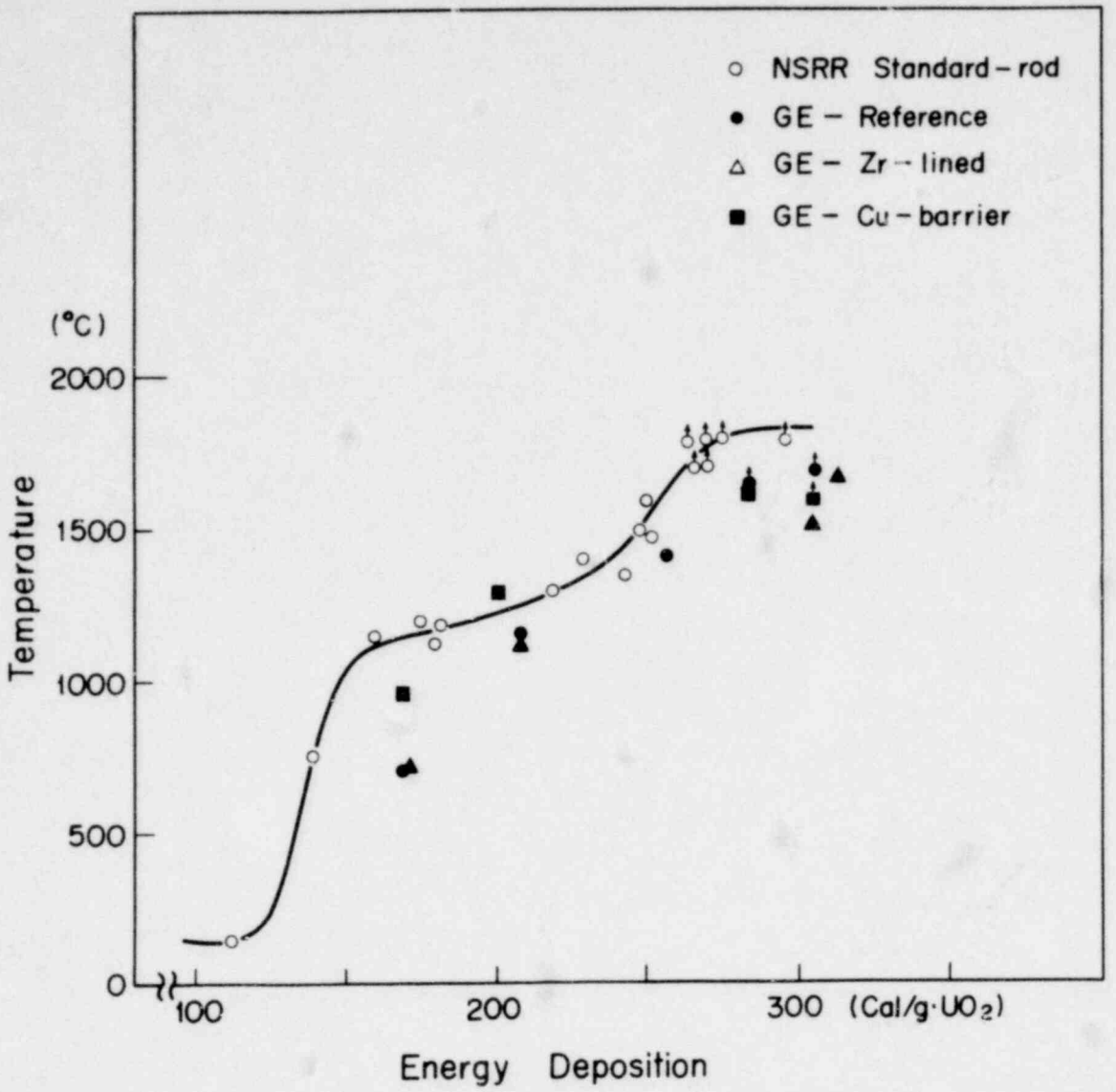

Fig.17 Max. Cladding Surface Temperature at Axial Center